



Published in final edited form as:

Free Radic Biol Med. 2017 November ; 112: 578–586. doi:10.1016/j.freeradbiomed.2017.08.026.

Loss of Nrf2 promotes alveolar type 2 cell loss in irradiated, fibrotic lung*

Geri Traver¹, Stacey Mont¹, David Gius², William E. Lawson³, George X. Ding¹, Konjeti R. Sekhar¹, and Michael L. Freeman^{1,*}

¹Department of Radiation Oncology, Vanderbilt University Medical Center, Nashville, TN 37232, USA

²Department of Radiation Oncology, Driskill Graduate Program in Life Sciences, Department of Pharmacology, Robert Lurie Cancer Center, Northwestern University Feinberg School of Medicine, Chicago, Illinois, USA

³Division of Pulmonary & Critical Care, Department of Medicine, Vanderbilt University Medical Center, Nashville, TN 37240

Abstract

The development of radiation-induced pulmonary fibrosis represents a critical clinical issue limiting delivery of therapeutic doses of radiation to non-small cell lung cancer. Identification of the cell types whose injury initiates a fibrotic response and the underlying biological factors that govern that response are needed for developing strategies that prevent or mitigate fibrosis. C57BL/6 mice (wild type, Nrf2 null, Nrf2^{flox/flox}, and Nrf2^{-/-}; SPC-Cre) were administered a thoracic dose of 12 Gy and allowed to recover for 250 days. Whole slide digital and confocal microscopy imaging of H&E, Masson's trichrome and immunostaining were used to assess tissue remodeling, collagen deposition and cell renewal/mobilization during the regenerative process. Histological assessment of irradiated, fibrotic wild type lung revealed significant loss of alveolar type 2 cells 250 days after irradiation. Type 2 cell loss and the corresponding development of fibrosis were enhanced in the Nrf2 null mouse. Yet, conditional deletion of Nrf2 in alveolar type 2 cells in irradiated lung did not impair type 2 cell survival nor yield an increased fibrotic phenotype. Instead, radiation-induced Np63 stem/progenitor cell mobilization was inhibited in the Nrf2 null mouse while the propensity for radiation-induced myofibroblasts derived from alveolar type 2 cells was magnified. In summary, these results indicate that Nrf2 is an important regulator of irradiated lung's capacity to maintain alveolar type 2 cells, whose injury can initiate a

*None of the authors has a conflict of interest.

Correspondence to ML Freeman, B902, TVC, Department of Radiation Oncology, Vanderbilt University Medical Center, Nashville, TN 37232, michael.freeman@vanderbilt.edu; 615-322-3606.

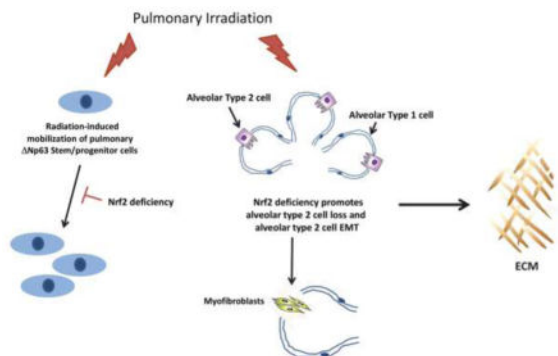
Author Contribution Statement:

GT, SM, WEL, KRS, DG and MLF designed the study. GT, SM, WEL, KRS and MLF performed the experiments. GXD performed the radiation dose calculations. All authors (GT, SM, WEL, KRS, DXG, and MLF) were involved in data interpretation, technical support, and writing the manuscript. All had final approval of the submitted manuscript.

Publisher's Disclaimer: This is a PDF file of an unedited manuscript that has been accepted for publication. As a service to our customers we are providing this early version of the manuscript. The manuscript will undergo copyediting, typesetting, and review of the resulting proof before it is published in its final citable form. Please note that during the production process errors may be discovered which could affect the content, and all legal disclaimers that apply to the journal pertain.

fibrotic phenotype. Loss of Nrf2 inhibits Np63 stem/progenitor mobilization, a key event for reconstitution of injured lung, while promoting a myofibroblast phenotype that is central for fibrosis.

Graphical abstract



Keywords

Nrf2; radiation; pulmonary fibrosis; alveolar type 2 cell; Np63

Introduction

Radiation therapy is used to treat approximately 900,000 lung cancer patients each year [1]. Research has shown that local tumor control and 5 year survival rates improve as the dose of radiation delivered to the tumor increases [1]. Normal tissue toxicity, however, limits this approach. The most common dose limiting adverse events are pulmonary pneumonitis and fibrosis [2]. Pneumonitis can develop within weeks of irradiation and in many, but not all cases is reversible. Fibrosis can develop months to years after treatment, is not reversible but progressive, and can lead to permanent impairment of lung function [2]. Currently, the biological factors that are critical for repair and renewal of distal epithelial tissue following radiation injury are incompletely understood. Identification of these factors represents an important step in reducing toxicity.

Nrf2, encoded by *Nfe2l2*, is a transcription factor [3] shown to regulate the expression of more than 400 genes [4], including those that encode antioxidant and drug-metabolizing enzymes [5]. Mont et. al. quantified *NFE2L2* mRNA expression in non-diseased tissue obtained from human lung and found a wide variation in constitutive *NFE2L2* mRNA expression [6]. When the data were divided into quartiles the results indicated that individuals in the 25th percentile expressed 11-fold less *NFE2L2* mRNA than those in the 75th percentile and this reduction correlated with loss of NRF2 target gene expression [6].

Loss of Nrf2 expression is associated with increased susceptibility to pulmonary fibrosis [7], including that produced by ionizing radiation [8]. Loss of Nrf2 expression can be a consequence of aging [9, 10], functional polymorphisms [11], and/or fibrotic TGF- β /pSmad3 signaling [12–15]. Preclinical models of pulmonary fibrosis indicate that Nrf2 is

suppressed as the disease progresses [16, 17] and that haploinsufficiency is sufficient for enhanced susceptibility [8]. Conversely, pirfenidone-mediated inhibition of pulmonary fibrosis does so in part by inducing expression of Nrf2 [18]. Hence, these data support a hypothesis that posits that loss of Nrf2 promotes pulmonary fibrosis.

An important question is the identification of irradiated cell types negatively impacted by loss of Nrf2. We reasoned that a prolonged period of recovery following irradiation would allow identification of cell types whose reparative process was impaired by loss of Nrf2. Using this strategy the lungs of wildtype and Nrf2 null C57BL/6 mice were administered 12 Gy. Assessing pulmonary injury 250 days after irradiation revealed that loss of Nrf2 significantly impeded alveolar type 2 cell recovery, a cell type that is central to the pathogenesis of non-radiation-induced pulmonary fibrosis [19–22]. Nrf2^{-/-}; SPC-Cre mice were used to determine if conditional loss of Nrf2 in alveolar type 2 cells directly impacted cell renewal following irradiation. Type 2 cell recovery from radiation-induced pulmonary injury was not impeded by disruption of the *Nfe2l2* gene. Pulmonary Np63 progenitor cell mobilization has the potential for generating type 2 cells following influenza infection or bleomycin-induced pulmonary injury [23–25]. Quantification of Np63 expressing cells revealed that mobilization of this progenitor cell occurred after radiation-induced pulmonary injury, but was diminished by loss of Nrf2. Myofibroblasts are responsible for the synthesis of pathogenic extracellular matrix proteins that define fibrosis and alveolar type 2 cell epithelial-to-mesenchymal transition (EMT) represents one pathway for their formation [26]. Remarkably, radiation-injury induced chronic type 2 cell EMT events that were amplified by an Nrf2 deficiency. Collectively these data suggest that the failure of alveolar type 2 cell numbers to recovery after irradiation is amplified by loss of Nrf2, which inhibits Np63 progenitor cell mobilization while driving type 2 cell transition to a myofibroblast phenotype.

Materials and Methods

Mice

Mice were maintained under specific pathogen free conditions. All procedures performed on animals were approved by the Institutional Animal Care and Use Committee at Vanderbilt University. C57BL/6 *Nfe2l2*^{-/-} mice (referred to as Nrf2 null) were originally generated by Chan et al [27] and have been backcrossed for more than 10 generations to C57BL/6j mice. Pleural effusion, which can be a confounding factor for survival studies [28] is not observed under our experimental conditions [8]. Generation of C57BL/6 *Nfe2l2*^{flox/flox} mice is described in Supplemental Materials and Methods. Congenic C57BL/6-*Gt(ROSA)26Sor^{tm4}(ACTB-tdTomato,-EGFP)Lox/j* (referred to as ROSA^{mT/mG} mice) were obtained from Jackson labs. *SFTPC-Cre* mouse were obtained from Dr. Brigid Hogan, Department of Cell Biology, Duke University School of Medicine. The *Nfe2l2*^{flox/flox} mice were crossed to the ROSA^{mT/mG} mice to generate *Nfe2l2*^{flox/flox}; ROSA^{mT/mG} mice that harbor undeleted Nrf2 floxed exons 4 and 5 (referred to as Nrf2^{flox/flox}). The *Nfe2l2*^{flox/flox}; ROSA^{mT/mG} mice were then crossed to *SFTPC-Cre* mice to generate *Nfe2l2*^{flox/flox}; ROSA^{mT/mG}; *SFTPC-Cre* mice in which Nrf2 is conditionally deleted in alveolar type 2 cells (referred to as Nrf2^{-/-}; SPC-Cre).

Irradiation

Ten to 12 week old male mice were randomly assigned to treatment groups. Isoflurane anesthetized mice were placed on a 37°C recirculating water heating pad and the thorax was administered 12 Gy (300 kVp/10 mA X-rays) at 1.64 Gy per min. With the exception of the thorax the entire animal was shielded by a custom lead block 2.5 cm thick.

Digital Histology

Whole slide imaging was performed in the Digital Histology Shared Resource at Vanderbilt University Medical Center (www.mc.vanderbilt.edu/dhsr). Formalin-fixed paraffin-embedded (FFPE) 5 μ m H&E stained sections or Masson's trichrome stained sections were imaged using a Leica SCN400 Slide scanner that provides high resolution wide field images ranging from 0.05x to 20x. Entire lung sections were first inspected at a low magnification. Figure S1A illustrates a 0.58x H&E image of an entire H&E stained lung section obtained 250 days after sham treatment of a wild type mouse. Following the initial inspection each entire lung section was then inspected at 20x. Figure S1B illustrates a 0.58x, 10x and 20x image of a lung section 250 days after irradiation of the lungs of a wild type mouse. Leica-associated software packages provide complex algorithms for unbiased, automated image quantitation of areas of interest. Tissue remodeling can be defined by changes in quantity, composition, and organization of structure [29]. For H&E stained sections remodeling was quantified as described by Ashcroft et al [30] and Hubner et al [31]. Image analysis was performed at 20x. The area occupied by tissue remodeling was quantified in μm^2 and expressed relative to the area of the entire field. A scale of 1–8 was employed [31]. Supplemental Table S1 summarizes the scale. The image analysis algorithms deconvolute Masson's trichrome stains, converting each stain into fluorescence pixels that can then be quantified in ImageJ.

Immunofluorescence staining and imaging

The following antibodies were used to immunostain FFPE sections: goat Spc (1:100; sc7706; Santa Cruz Biotechnology); rabbit Spc (1:500; ab3786; Millipore); rabbit Pdpn (1:100; sc134483; Santa Cruz Biotechnology); rabbit 53BP1 (1:3500; NB100-304; Novus Biologicals); goat CD34 (1:100; Santa Cruz Biotechnology); rabbit eGFP (1:1000; TA150032; Origene); mouse α SMA (1:3000; A2547; Sigma Aldrich); rabbit Np63 (1:100; 619001; Biolegend); donkey anti-goat Alexa 568 (1:2000; A11057; Thermo Fisher Scientific); goat anti-rabbit Alexa 647 (1:2000, A21244; Thermo Fisher Scientific); donkey anti-mouse (1:2000; A31571; Thermo Fisher Scientific). All sections were counterstained with DAPI. Whole slide immunofluorescence imaging was performed in the Digital Histology Shared Resource at Vanderbilt University Medical Center using a Leica Apero Versa whole slide scanner that provides high resolution wide field images of ranging from 0.05x to 40x. Entire lung sections were first inspected at a low magnification. Following the initial inspection each entire lung section was then inspected at 20 to 40x. Images were captured as jpeg files. Confocal images of immunofluorescence staining were acquired using an Olympus FV-1000 inverted confocal microscope using a 60x/1.45 Plan-Apochromat oil immersion objective lens. Images were captured as jpeg files.

Immunofluorescence intensity quantification

ImageJ software was used to quantify fluorescence intensity. Antibody-specific immunofluorescence intensity per field was calculated using ImageJ (NIH) and corrected for DAPI staining per field in order to account for tissue cellularity. Background staining was quantified and mean background staining was subtracted from antibody-specific immunofluorescence intensity. We report mean relative intensity \pm SD, which is defined as (antibody-specific immunofluorescence intensity corrected for DAPI staining per field) minus mean background staining. Mean relative intensity of sham control is reported as 1.0.

Statistical Analysis

An unpaired t test or an analysis of variance was used for comparison between various groups. A *P* value less than 0.05 was considered statistically significant.

Results

Loss of Nrf2 potentiates tissue remodeling and increases formation of fibrotic foci

Previously, we reported that an Nrf2 deficiency increased radiation-induced lung injury to a greater extent in male C57BL/6 mice compared female mice [8]. Based on this knowledge we chose to use male mice in this investigation and administer a thoracic dose of 12 Gy, a dose that produces a mortality rate of less than 10% [32]. A 250 day recovery period was used in order to provide sufficient time for repair and regeneration of irradiated cells.

The degree of radiation-induced tissue remodeling was quantified from H&E stained sections while Masson's trichrome staining was used to assess collagen deposition (Figure 1). Irradiation produced tissue remodeling and collagen deposition in wild type and Nrf2 deficient lung compared to sham-treated mice (Figure 1A vs C; E vs G, B vs D, and F vs H). Nrf2 null mice were 1.6 fold more susceptible to radiation-induced lung injury compared to wild type mice, as measured by tissue remodeling ($P=0.0002$; $N=10$ mice, 112 fields; Figure 1, C vs D) or collagen deposition ($P=0.036$; $N=10$ mice, 71 fields; Figure 1, G vs H).

Assessing endothelial versus epithelial recovery following irradiation

We examined alveoli 250 days after irradiation, assessing recovery of cell types thought to be critical for the reparative process. Pulmonary capillary endothelial cells can be crucial for regrowth/regeneration of injured alveoli [33, 34]. Endothelial cell injury is observed within hours following administration of radiation doses that produce rodent mortality rates that approach 100%. Under such conditions it is hypothesized that endothelial injury may contribute to radiation-mediated pulmonary dysfunction [35–37]. However, it is not known if alveolar endothelial cell injury is a key factor for the development of pulmonary fibrosis following doses of radiation that produce mortality rates of less than 10%. To address this question we quantified alveolar endothelial cells following administration of 12 Gy ($LD_{50/180} < 10\%$) to the thorax of wild type and Nrf2 null mice. Podoplanin (Pdpn) immunofluorescence was used to identify alveolar type I cells (Figure S2). CD31 immunofluorescence was used to identify endothelial cells in alveoli. Representative images are shown in Figure S2A. The analysis revealed that 250 days after irradiation there was a

small but statistically significant 25% decrease in CD31 immunostaining compared to sham ($P = 0.008$, $N = 20$ mice, 148 fields) but that CD31 immunostaining in irradiated lung was independent of Nrf2 ($P > 0.05$, $N = 10$ mice, 99 fields, Figure S2B).

Alveolar type 2 cells are surfactant producing, self-renewing stem cells that can differentiate into type 1 cells [38]. There is compelling evidence that failure of type 2 cells to recover from injury is sufficient to induce pulmonary fibrosis in non-radiation models [19–22]. The question of whether alveolar type 2 cells recover and regenerate following radiation injury has not been resolved. Almedia et al [39] administered 12 Gy to the lungs of female FVB/N mice and assessed Spc expression 98 days later. They found approximately twice as many alveolar type 2 cells in irradiated lung compared to sham. Citrin et al [40] irradiated C57BL/6 mice with 1 7.5 Gy or 5 fractions of 5 Gy or 6 Gy. Sixteen weeks after irradiation there was a 2-fold decrease in type 2 cells [40]. To address this question Pdpn immunofluorescence was again used to identify alveoli type 1 cells. Spc immunofluorescence was used to quantify the presence of alveolar type 2 cells (Figure 2). Two hundred fifty days after irradiation of wild type mice there was a 2 fold loss of alveolar type 2 cells compared to sham-treated lung ($P = 0.0037$, $N = 10$ mice, 96 fields). In irradiated Nrf2 null mice there was a 4 fold loss of alveolar type 2 cells compared to sham treated lung ($P = 0.0002$, $N = 10$ mice, 77 fields). The analysis revealed a significant radiation-induced loss of alveolar type 2 cells that was compounded by loss of Nrf2 ($P = 0.0023$, $N = 10$ mice, 98 fields, Figure 2).

Expression of the DNA repair protein 53BP1 is not affected by loss of Nrf2

McDonald et al [41] have shown that proliferating Nrf2 null MEFs are radiosensitive. *Tp53bp1* encodes the DNA repair protein 53BP1 and contains an Antioxidant Response Element (ARE) in its proximal promoter [42]. Therefore, we asked whether loss of Nrf2 would diminish constitutive 53BP1 expression. Lung sections from sham and irradiated wild type and Nrf2 null mice were immunostained for 53BP1 and Spc (Figure S3A & S3B). 53BP1 immunofluorescence per cell in sham ($P > 0.05$) and irradiated lung ($P = 0.66$) was found to be independent of genotype. Lung sections were also stained for the catalytic subunit of glutamate-cysteine ligase encoded by the gene *Gclc* as a positive control (Figure S3C). Constitutive and inducible *Gclc* expression are governed by AREs [43]. *Gclc* expression was not observed in Nrf2 null lung.

Conditional disruption of *Nfe2l2* in alveolar type 2 cells

Type 2 cell repopulation following cytotoxic injury is dependent on the severity of injury [23] and is a consequence of alveolar type 2 self-renewal capacity [38], as well as regeneration by progenitor Club cells [44] and transdifferentiation of Hopx+ alveolar type 1 cells [45]. In addition to these cell types it has been reported that distal airway stem cells/lineage negative Np63 progenitor cells are essential for lung regeneration following injury [23, 24]. Under oxygenated conditions Np63 cells have the potential for proliferative expansion and differentiation into type 1 and 2 cells [24]. Under hypoxic conditions HIF α expression promotes Krt5 basal cell-like metaplasia [25].

We first investigated type 2 cell self-renewal. Mice with conditional deletion of Nrf2 in alveolar type 2 cells (Nrf2^{-/-}; *SPC-Cre*) and control Nrf2^{flx/flx} mice (Supplemental Figure 4), as well as control *ROSA^{mTmG}*; *SFTPC-Cre* mice were used to determine if alveolar type 2 cell hypersensitivity observed in irradiated Nrf2 null mice was a direct consequence of loss of Nrf2 in the type 2 cells. We quantified tissue remodeling by H&E staining in sham-treated and irradiated (12 Gy) mice 250 days after irradiation. Conditional loss of Nrf2 in alveolar type 2 cells did not enhance radiation-mediated tissue remodeling ($P = 0.78$, Figures 3A & 3B). The degree of radiation tissue remodeling was essentially the same for *ROSA^{mTmG}*; *SFTPC-Cre*, Nrf2^{flx/flx} and Nrf2^{-/-}; *SPC-Cre* mice.

Next, we asked whether conditional loss of Nrf2 in type 2 cells affected recovery of these cells after radiation injury. Pdpn immunofluorescence was used to identify alveoli type I cells. Spc immunofluorescence was used to quantify the presence of alveolar type 2 cells 250 days after administration of 12 Gy. Loss of Nrf2 in type 2 cells did not affect cell recovery ($P = 0.73$, Figures 3C & 3D).

Np63 lineage-negative progenitor cell mobilization is suppressed by loss of Nrf2 in irradiated lung

As stated above, Np63 lineage-negative progenitor cell mobilization is critical for cell recover following certain types of pulmonary injury [23, 24]. However, it was not known whether Np63 mobilization occurred following lung irradiation. Therefore, we quantified Np63 expression in sham and irradiated lung 250 days after treatment (Figure 4). Np63 mobilization was observed in irradiated wild type lung relative to sham treatment ($P < 0.0001$, $N = 90$ fields, 9 mice), consistent with the concept that mobilization occurs in injured lung [24]. What is surprising is that mobilization continues so long after injury, supporting the concept that radiation injury produces a progressive pathophysiology. While we cannot exclude mobilization in Nrf2 null lung prior to sacrifice, Np63 mobilization was not observed in irradiated Nrf2 null lung relative to sham ($P > 0.05$, $N = 88$ fields, 9 mice) or to irradiated wild type lung 250 days after irradiation ($P < 0.006$, 89 fields, $N = 9$ mice). This observation leads us to hypothesize that loss of Np63 mobilization in the Nrf2 null lung may account, in part, for the loss of alveolar type 2 cells observed in irradiated null lung.

Radiation-induced epithelial-to-mesenchymal transition (EMT)

Myofibroblasts represent a primary source for collagen deposition [46] and can be derived from resident fibroblasts, alveolar type 2 cells that undergo an epithelial-to-mesenchymal transition (EMT), and fibrocytes [47]. Epithelial cells express both epithelial and mesenchymal markers as they transition into a mesenchymal phenotype. While Rock et al [47] found no evidence for EMT events following bleomycin-induced pulmonary fibrosis, Bali et al [26] reported that alveolar type 2 cells can undergo EMTs following radiation injury and Zhou et al [48] found that Nrf2 suppressed TGF β -mediated EMT events in a rat alveolar type 2 cell culture model. Thus, it was of interest to determine if loss of Nrf2 would promote type 2 cell EMT events following radiation injury. Lung sections from wild type and Nrf2 null mice were immunostained with antibody to Spc in order to identify alveolar type 2 cells and antibody to α SMA [47] for identification of a mesenchymal transition [47].

Inspection of immunofluorescence in irradiated lung sections revealed that the majority of alveolar type 2 cells (characterized by Spc immunostaining surrounding a DAPI stained nucleus) did not express α SMA (compare Figures 5B & 5C). Remarkably, 250 days after irradiation a small percentage of cells exhibited DAPI stained nuclei that were surrounded by both Spc and α SMA (Figure 5D). The frequency of such events 250 days after irradiation is shown in Figure 5E for wild type and Nrf2 null mice. Loss of Nrf2 resulted in a 10 fold increase in EMT events ($P= 0.045$, $N = 8$ mice).

Examination of immunofluorescence by confocal imaging of multiple optical sections was used to validate alveolar type 2 co-expression of the epithelial Spc marker and the α SMA mesenchymal marker [47]. The images obtained from Nrf2 null sham treated lung shown in Figure 6A illustrate four of nine Z stack slices, 0.58 μ m each. None of the cells (denoted by DAPI nuclei) in Panel A co-express Spc and α SMA. The images shown in Panel B were obtained from Nrf2 null irradiated lung and represent a single 0.58 μ m slice, labelled 5357.96 μ m. Two of the nuclei shown in Panel B express both Spc and α SMA (denoted by white arrows). Slice Z 5359.12 μ m (Panel C) illustrates the same two nuclei imaged 1.16 μ m from section Z5357.96 μ m. In this slice these two nuclei denoted by white arrows again express both Spc and α SMA. These results indicate that there are ongoing, persistent EMT events that occur long after irradiation of lung.

Discussion

The object of radiation therapy is to deliver a definitive dose to tumor while minimizing the dose delivered to the surrounding normal tissue [49]. Although normal tissue toxicity defines the therapeutic dose, the biological factors that impact toxicity are not well characterized [49]. Identification of these factors on an individualized patient basis would allow personalized dose delivery, thereby increasing the potential for controlling tumor growth. The problem of normal tissue toxicity is particularly acute for locally advanced non-small cell lung cancer [50], with pulmonary fibrosis representing one of several normal tissue complications that can develop after irradiation of the lung. It is thought to be initiated by cell injury that is followed by reprogramming that subsequently drives myofibroblast deposition of extracellular matrix [51].

A goal of this investigation was to identify cell types whose recovery was impaired by loss of Nrf2. Therefore a dose of 12 Gy was administered to the lung. A recovery period of 250 days was employed in order to allow sufficient time for repair of the radiation damage and for subsequent stem/progenitor cell regeneration of injured tissue. The observation that 12 Gy produced epithelium remodeling and collagen deposition indicates an inability to fully repair and regenerate, an outcome that was significantly enhanced in the Nrf2 null mouse.

An Nrf2 deficiency would be expected to produce pleiotropic pathophysiological effects in irradiated lung due to the fact that Nrf2 regulates expression of over 400 genes [4]. Loss of Nrf2 has been shown to increase the radiation sensitivity of proliferating cells [41] [52]. Yet, the alveolar capillary network was able to recover and the degree of recovery was not impaired by loss of Nrf2. These results are in contrast to the reports by others who found that radiation doses that caused significant animal mortality limited recovery of pulmonary

endothelial cells [35–37]. On the other hand, alveolar type 2 cells were not able to implement full recovery following absorption of 12 Gy and this failure to recover was coincident with increased tissue remodeling and collagen deposition. Given that injury to alveolar type 2 cells, which are considered stem/progenitor cells [47], is sufficient for inducing a fibrosis phenotype in several model systems [19–22], our data suggest that radiation-induced loss of these cells, along with type 2 cell senescence [40], represent underlying initiating mechanisms responsible for radiation pulmonary injury. Further support for this hypothesis is provided by Balli et al [26] who expressed constitutively active *Foxm1* in alveolar type 2 cells using a SPC-inducible promoter. Expression of the *Foxm1* transgene in irradiated lung (12 Gy) induced an EMT phenotype in type 2 cells, shortened the time for the development of radiation-induced fibrosis and increased the severity of fibrosis compared to irradiated lung that did not express the transgene. To complement these studies the authors conditionally deleted *Foxm1* from type 2 cells and observed diminished radiation-induced fibrosis. These data demonstrate that reprogramming of alveolar type 2 cells significantly affects radiation-induced pulmonary fibrosis.

Conditional deletion of *Nfe2l2* in alveolar type 2 cells was not sufficient for enhancement of radiation-induced pulmonary injury, indicating that the *Nrf2* deficiency did not significantly radiosensitize type 2 cells nor impair type 2 cell self-renewal. Type 2 cell renewal is also a function of Club progenitor cell differentiation [40] and/or transdifferentiation of *Hopx*+ alveolar type 1 cells [41]. In addition, under conditions of mild pulmonary injury that do not induce hypoxia *Np63* progenitor cells may contribute [24, 25].

We observed *Np63* lineage-negative progenitor cell mobilization 250 days after radiation injury, implying that mobilization is also a response to pulmonary injury induced by ionizing radiation. While we cannot exclude mobilization prior to 250 days, *Np63* mobilization was not observed in *Nrf2* null mice at this recovery interval. Vaughan et al reported that after bleomycin injury there is an expansion of *Krf5*+ *Np63* cells, 30% of which resolve into alveolar type 2 cells [23]. *Np63* progenitor cell differentiation into type 2 cells requires *Wnt* signaling [25] that can be suppressed by oxidative stress [53], a key feature of an *Nrf2* deficiency. Thus, one interpretation for these data is that failure to mobilize *Np63* progenitor cells in the *Nrf2* null mouse may be a consequence of increased oxidant stress and may account, in part, for the loss of type 2 cells in irradiated *Nrf2* null mice.

The myofibroblast phenotype is considered a consequence of alveolar injury [51]. Myofibroblasts can originate from resident fibroblasts, alveolar type 2 cells that undergo an EMT, and fibrocytes [47]. Based on the work of Bali et al [26] and Zhou et al [48] we focused on type 2 cell EMT events. The data clearly indicate the presence of EMTs occurring 250 days after irradiation, with greater frequency in the *Nrf2* null mouse. These data are consistent with the knowledge that radiation-induced epithelial injury results in chronic overexpression of *TGF- β* [54] and connective tissue growth factor (CTFG) [55], two cytokines that have major roles in myofibroblast formation. Furthermore it is known that the expression of these cytokines is enhanced in the *Nrf2* null mouse following injury [16, 56] and thus may account for the increase in EMT events and the concomitant loss of type 2 cells observed in this genotype.

In summary, our data support the concept that injury to alveolar type 2 cells is a critical event in the pathogenesis of pulmonary fibrosis. We provide evidence that Nrf2 is crucial for recovery from radiation-induced pulmonary injury and specifically for alveolar type 2 cells. Diminished expression of Nrf2 in irradiated lung may impair mobilization of critical Np63 progenitor cells, thereby diminishing alveolar type 2 cell recovery while promoting EMTs in alveolar type 2 cells.

Supplementary Material

Refer to Web version on PubMed Central for supplementary material.

Acknowledgments

This study was supported in part by RO1 HL112286 (MLF), T32CA093240 (MLF), 2R01CA152601, 1R01CA152799, 1R01CA168292, 1R01CA214025, the Avon Foundation for Breast Cancer Research, the Lynn Sage Cancer Research Foundation, the Zell Family Foundation, and the Chicago Biomedical Consortium, and the Searle Funds at The Chicago Community Trust (DG), Vanderbilt-Ingram Cancer CTR Grant P30 CA68485, Additional support for experiments performed using the VUMC Cell Imaging Shared Resource was provided in part by CA68485, DK20593, DK58404, HD15052, DK59637 and EY08126.

References

1. Kong FM, Ao X, Wang L, Lawrence TS. The use of blood biomarkers to predict radiation lung toxicity: a potential strategy to individualize thoracic radiation therapy. *Cancer Control*. 2008; 15:140–150. [PubMed: 18376381]
2. Kong FM, Wang S. Nondosimetric risk factors for radiation-induced lung toxicity. *Semin Radiat Oncol*. 2015; 25:100–109. [PubMed: 25771414]
3. Moi P, Chan K, Asunis I, Cao A, Kan YW. Isolation of NF-E2-related factor 2 (Nrf2), a NF-E2-like basic leucine zipper transcriptional activator that binds to the tandem NF-E2/AP1 repeat of the beta-globin locus control region. *Proc Natl Acad Sci U S A*. 1994; 91:9926–9930. [PubMed: 7937919]
4. Malhotra D, Portales-Casamar E, Singh A, Srivastava S, Arenillas D, Happel C, Shyr C, Wakabayashi N, Kensler TW, Wasserman WW, Biswal S. Global mapping of binding sites for Nrf2 identifies novel targets in cell survival response through ChIP-Seq profiling and network analysis. *Nucleic acids research*. 2010; 38:5718–5734. [PubMed: 20460467]
5. Hayes JD, Dinkova-Kostova AT. The Nrf2 regulatory network provides an interface between redox and intermediary metabolism. *Trends Biochem Sci*. 2014; 39:199–218. [PubMed: 24647116]
6. Mont S, Davies SS, Roberts LJ Second, Mernaugh RL, McDonald WH, Segal BH, Zackert W, Kropski JA, Blackwell TS, Sekhar KR, Galligan JJ, Massion PP, Marnett LJ, Travis EL, Freeman ML. Accumulation of isolevuglandin-modified protein in normal and fibrotic lung. *Sci Rep*. 2016; 6:24919. [PubMed: 27118599]
7. Zhao H, Eguchi S, Alam A, Ma D. The role of nuclear factor-erythroid 2 related factor 2 (Nrf-2) in the protection against lung injury. *Am J Physiol Lung Cell Mol Physiol*. 2017; 312:L155–L162. [PubMed: 27864288]
8. Travis EL, Rachakonda G, Zhou X, Korhonen K, Sekhar KR, Biswas S, Freeman ML. NRF2 deficiency reduces life span of mice administered thoracic irradiation. *Free Radic Biol Med*. 2011; 51:1175–1183. [PubMed: 21712086]
9. Soundararajan R, Stearns TM, Czachor A, Fukumoto J, Turn C, Westermann-Clark E, Breitzig M, Tan L, Lockey RF, King BL, Kolliputi N. Global gene profiling of aging lungs in Atp8b1 mutant mice. *Aging (Albany NY)*. 2016; 8:2232–2252. [PubMed: 27689529]
10. Swamy SM, Rajasekaran NS, Thannickal VJ. Nuclear Factor-Erythroid-2-Related Factor 2 in Aging and Lung Fibrosis. *Am J Pathol*. 2016; 186:1712–1723. [PubMed: 27338106]
11. Marzec JM, Christie JD, Reddy SP, Jedlicka AE, Vuong H, Lancken PN, Aplenc R, Yamamoto T, Yamamoto M, Cho HY, Kleeberger SR. Functional polymorphisms in the transcription factor

- NRF2 in humans increase the risk of acute lung injury. *FASEB J.* 2007; 21:2237–2246. [PubMed: 17384144]
12. Kim JY, Kim YS, Kim YK, Park HJ, Kim SJ, Kang JH, Wang YP, Jang HS, Lee SN, Yoon SC. The TGF-beta1 dynamics during radiation therapy and its correlation to symptomatic radiation pneumonitis in lung cancer patients. *Radiat Oncol.* 2009; 4:59. [PubMed: 19943923]
 13. Rube CE, Uthe D, Schmid KW, Richter KD, Wessel J, Schuck A, Willich N, Rube C. Dose-dependent induction of transforming growth factor beta (TGF-beta) in the lung tissue of fibrosis-prone mice after thoracic irradiation. *Int J Radiat Oncol Biol Phys.* 2000; 47:1033–1042. [PubMed: 10863076]
 14. Kang JH, Jung MY, Yin X, Andrianifahanana M, Hernandez DM, Leof EB. Cell-penetrating peptides selectively targeting SMAD3 inhibit profibrotic TGF-beta signaling. *J Clin Invest.* 2017
 15. Bakin AV, Stourman NV, Sekhar KR, Rinehart C, Yan X, Meredith MJ, Arteaga CL, Freeman ML. Smad3-ATF3 signaling mediates TGF-beta suppression of genes encoding Phase II detoxifying proteins. *Free Radic Biol Med.* 2005; 38:375–387. [PubMed: 15629866]
 16. Kalash R, Berhane H, Au J, Rhieu BH, Epperly MW, Goff J, Dixon T, Wang H, Zhang X, Franicola D, Shinde A, Greenberger JS. Differences in irradiated lung gene transcription between fibrosis-prone C57BL/6NHsd and fibrosis-resistant C3H/HeNHsd mice. *In Vivo.* 2014; 28:147–171. [PubMed: 24632969]
 17. Hecker L, Logsdon NJ, Kurundkar D, Kurundkar A, Bernard K, Hock T, Meldrum E, Sanders YY, Thannickal VJ. Reversal of persistent fibrosis in aging by targeting Nox4-Nrf2 redox imbalance. *Sci Transl Med.* 2014; 6:231ra247.
 18. Liu Y, Lu F, Kang L, Wang Z, Wang Y. Pirfenidone attenuates bleomycin-induced pulmonary fibrosis in mice by regulating Nrf2/Bach1 equilibrium. *BMC Pulm Med.* 2017; 17:63. [PubMed: 28420366]
 19. Liang J, Zhang Y, Xie T, Liu N, Chen H, Geng Y, Kurkciyan A, Mena JM, Stripp BR, Jiang D, Noble PW. Hyaluronan and TLR4 promote surfactant-protein-C-positive alveolar progenitor cell renewal and prevent severe pulmonary fibrosis in mice. *Nat Med.* 2016; 22:1285–1293. [PubMed: 27694932]
 20. Povedano JM, Martinez P, Flores JM, Mulero F, Blasco MA. Mice with Pulmonary Fibrosis Driven by Telomere Dysfunction. *Cell Rep.* 2015; 12:286–299. [PubMed: 26146081]
 21. Wang R, Ibarra-Sunga O, Verlinski L, Pick R, Uhal BD. Abrogation of bleomycin-induced epithelial apoptosis and lung fibrosis by captopril or by a caspase inhibitor. *Am J Physiol Lung Cell Mol Physiol.* 2000; 279:L143–151. [PubMed: 10893213]
 22. Winters CJ, Koval O, Murthy S, Allamargot C, Sebag SC, Paschke JD, Jaffer OA, Carter AB, Grumbach IM. CaMKII inhibition in type II pneumocytes protects from bleomycin-induced pulmonary fibrosis by preventing Ca²⁺-dependent apoptosis. *Am J Physiol Lung Cell Mol Physiol.* 2016; 310:L86–94. [PubMed: 26545899]
 23. Vaughan AE, Brumwell AN, Xi Y, Gotts JE, Brownfield DG, Treutlein B, Tan K, Tan V, Liu FC, Looney MR, Matthay MA, Rock JR, Chapman HA. Lineage-negative progenitors mobilize to regenerate lung epithelium after major injury. *Nature.* 2015; 517:621–625. [PubMed: 25533958]
 24. Zuo W, Zhang T, Wu DZ, Guan SP, Liew AA, Yamamoto Y, Wang X, Lim SJ, Vincent M, Lessard M, Crum CP, Xian W, McKeon F. p63(+)Krt5(+) distal airway stem cells are essential for lung regeneration. *Nature.* 2015; 517:616–620. [PubMed: 25383540]
 25. Xi Y, Kim T, Brumwell AN, Driver IH, Wei Y, Tan V, Jackson JR, Xu J, Lee DK, Gotts JE, Matthay MA, Shannon JM, Chapman HA, Vaughan AE. Local lung hypoxia determines epithelial fate decisions during alveolar regeneration. *Nat Cell Biol.* 2017; 19:904–914. [PubMed: 28737769]
 26. Balli D, Ren X, Chou FS, Cross E, Zhang Y, Kalinichenko VV, Kalin TV. Foxm1 transcription factor is required for macrophage migration during lung inflammation and tumor formation. *Oncogene.* 2012; 31:3875–3888. [PubMed: 22139074]
 27. Chan K, Lu R, Chang JC, Kan YW. NRF2, a member of the NFE2 family of transcription factors, is not essential for murine erythropoiesis, growth, and development. *Proc Natl Acad Sci U S A.* 1996; 93:13943–13948. [PubMed: 8943040]

28. Jackson IL, Vujaskovic Z, Down JD. Revisiting strain-related differences in radiation sensitivity of the mouse lung: recognizing and avoiding the confounding effects of pleural effusions. *Radiat Res.* 2010; 173:10–20. [PubMed: 20041755]
29. VINAY, KUMAR, AKA., FAUSTO, NELSON. *Robbins and Cotran Pathological Basis of Disease.* 7. New York: Elsevier Saunders; 2005.
30. Ashcroft T, Simpson JM, Timbrell V. Simple method of estimating severity of pulmonary fibrosis on a numerical scale. *J Clin Pathol.* 1988; 41:467–470. [PubMed: 3366935]
31. Hubner RH, Gitter W, El Mokhtari NE, Mathiak M, Both M, Bolte H, Freitag-Wolf S, Bewig B. Standardized quantification of pulmonary fibrosis in histological samples. *Biotechniques.* 2008; 44:507–511. 514–507. [PubMed: 18476815]
32. Jackson IL, Xu PT, Nguyen G, Down JD, Johnson CS, Katz BP, Hadley CC, Vujaskovic Z. Characterization of the dose response relationship for lung injury following acute radiation exposure in three well-established murine strains: developing an interspecies bridge to link animal models with human lung. *Health Phys.* 2014; 106:48–55. [PubMed: 24276549]
33. Ding BS, Nolan DJ, Guo P, Babazadeh AO, Cao Z, Rosenwaks Z, Crystal RG, Simons M, Sato TN, Worgall S, Shido K, Rabbany SY, Raffi S. Endothelial-derived angiocrine signals induce and sustain regenerative lung alveolarization. *Cell.* 2011; 147:539–553. [PubMed: 22036563]
34. Raffi S, Cao Z, Lis R, Siempos, Chavez D, Shido K, Rabbany SY, Ding BS. Platelet-derived SDF-1 primes the pulmonary capillary vascular niche to drive lung alveolar regeneration. *Nat Cell Biol.* 2015; 17:123–136. [PubMed: 25621952]
35. Phillips TL. An ultrastructural study of the development of radiation injury in the lung. *Radiology.* 1966; 87:49–54. [PubMed: 5940475]
36. Penney DP, Rubin P. Specific early fine structural changes in the lung irradiation. *Int J Radiat Oncol Biol Phys.* 1977; 2:1123–1132. [PubMed: 599063]
37. Kolesnick R, Fuks Z. Radiation and ceramide-induced apoptosis. *Oncogene.* 2003; 22:5897–5906. [PubMed: 12947396]
38. Barkauskas CE, Cronce MJ, Rackley CR, Bowie EJ, Keene DR, Stripp BR, Randell SH, Noble PW, Hogan BL. Type 2 alveolar cells are stem cells in adult lung. *J Clin Invest.* 2013; 123:3025–3036. [PubMed: 23921127]
39. Almeida C, Nagarajan D, Tian J, Leal SW, Wheeler K, Munley M, Blackstock W, Zhao W. The role of alveolar epithelium in radiation-induced lung injury. *PLoS One.* 2013; 8:e53628. [PubMed: 23326473]
40. Citrin DE, Shankavaram U, Horton JA, Shield W 3rd, Zhao S, Asano H, White A, Sowers A, Thetford A, Chung EJ. Role of type II pneumocyte senescence in radiation-induced lung fibrosis. *J Natl Cancer Inst.* 2013; 105:1474–1484. [PubMed: 24052614]
41. McDonald JT, Kim K, Norris AJ, Vlashi E, Phillips TM, Lagadec C, Della Donna L, Ratikan J, Szelag H, Hlatky L, McBride WH. Ionizing radiation activates the Nrf2 antioxidant response. *Cancer Res.* 2010; 70:8886–8895. [PubMed: 20940400]
42. Kim SB, Pandita RK, Eskiocak U, Ly P, Kaisani A, Kumar R, Cornelius C, Wright WE, Pandita TK, Shay JW. Targeting of Nrf2 induces DNA damage signaling and protects colonic epithelial cells from ionizing radiation. *Proc Natl Acad Sci U S A.* 2012; 109:E2949–2955. [PubMed: 23045680]
43. Mulcahy RT, Wartman MA, Bailey HH, Gipp JJ. Constitutive and beta-naphthoflavone-induced expression of the human gamma-glutamylcysteine synthetase heavy subunit gene is regulated by a distal antioxidant response element/TRE sequence. *J Biol Chem.* 1997; 272:7445–7454. [PubMed: 9054446]
44. Zheng D, Limmon GV, Yin L, Leung NH, Yu H, Chow VT, Chen J. Regeneration of alveolar type I and II cells from Scgblal-expressing cells following severe pulmonary damage induced by bleomycin and influenza. *PLoS One.* 2012; 7:e48451. [PubMed: 23119022]
45. Jain R, Barkauskas CE, Takeda N, Bowie EJ, Aghajanian H, Wang Q, Padmanabhan A, Manderfield LJ, Gupta M, Li D, Li L, Trivedi CM, Hogan BL, Epstein JA. Plasticity of Hopx(+) type I alveolar cells to regenerate type II cells in the lung. *Nat Commun.* 2015; 6:6727. [PubMed: 25865356]

46. Phan SH. The myofibroblast in pulmonary fibrosis. *Chest*. 2002; 122:286S–289S. [PubMed: 12475801]
47. Rock JR, Barkauskas CE, Cronic MJ, Xue Y, Harris JR, Liang J, Noble PW, Hogan BL. Multiple stromal populations contribute to pulmonary fibrosis without evidence for epithelial to mesenchymal transition. *Proc Natl Acad Sci U S A*. 2011; 108:E1475–1483. [PubMed: 22123957]
48. Zhou W, Mo X, Cui W, Zhang Z, Li D, Li L, Xu L, Yao H, Gao J. Nrf2 inhibits epithelial-mesenchymal transition by suppressing snail expression during pulmonary fibrosis. *Sci Rep*. 2016; 6:38646. [PubMed: 27982105]
49. Barnett GC, West CM, Dunning AM, Elliott RM, Coles CE, Pharoah PD, Burnet NG. Normal tissue reactions to radiotherapy: towards tailoring treatment dose by genotype. *Nat Rev Cancer*. 2009; 9:134–142. [PubMed: 19148183]
50. Bradley JD, Paulus R, Komaki R, Masters G, Blumenschein G, Schild S, Bogart J, Hu C, Forster K, Magliocco A, Kavadi V, Garces YI, Narayan S, Iyengar P, Robinson C, Wynn RB, Koprowski C, Meng J, Beitler J, Gaur R, Curran W Jr, Choy H. Standard-dose versus high-dose conformal radiotherapy with concurrent and consolidation carboplatin plus paclitaxel with or without cetuximab for patients with stage IIIA or IIIB non-small-cell lung cancer (RTOG 0617): a randomised, two-by-two factorial phase 3 study. *Lancet Oncol*. 2015; 16:187–199. [PubMed: 25601342]
51. Blackwell TS, Tager AM, Borok Z, Moore BB, Schwartz DA, Anstrom KJ, Bar-Joseph Z, Bitterman P, Blackburn MR, Bradford W, Brown KK, Chapman HA, Collard HR, Cosgrove GP, Deterding R, Doyle R, Flaherty KR, Garcia CK, Hagood JS, Henke CA, Herzog E, Hogaboam CM, Horowitz JC, King TE Jr, Loyd JE, Lawson WE, Marsh CB, Noble PW, Noth I, Sheppard D, Olsson J, Ortiz LA, O’Riordan TG, Oury TD, Raghu G, Roman J, Sime PJ, Sisson TH, Tschumperlin D, Violette SM, Weaver TE, Wells RG, White ES, Kaminski N, Martinez FJ, Wynn TA, Thannickal VJ, Eu JP. Future directions in idiopathic pulmonary fibrosis research. An NHLBI workshop report. *Am J Respir Crit Care Med*. 2014; 189:214–222. [PubMed: 24160862]
52. Jayakumar S, Pal D, Sandur SK. Nrf2 facilitates repair of radiation induced DNA damage through homologous recombination repair pathway in a ROS independent manner in cancer cells. *Mutat Res*. 2015; 779:33–45. [PubMed: 26133502]
53. Shin SY, Kim CG, Jho EH, Rho MS, Kim YS, Kim YH, Lee YH. Hydrogen peroxide negatively modulates Wnt signaling through downregulation of beta-catenin. *Cancer Lett*. 2004; 212:225–231. [PubMed: 15279902]
54. Yi ES, Bedoya A, Lee H, Chin E, Saunders W, Kim SJ, Danielpour D, Remick DG, Yin S, Ulich TR. Radiation-induced lung injury in vivo: expression of transforming growth factor-beta precedes fibrosis. *Inflammation*. 1996; 20:339–352. [PubMed: 8872498]
55. Bickelhaupt S, Erbel C, Timke C, Wirkner U, Dadrich M, Flechsig P, Tietz A, Pfohler J, Gross W, Peschke P, Hoeltgen L, Katus HA, Grone HJ, Nicolay NH, Saffrich R, Debus J, Sternlicht MD, Seeley TW, Lipson KE, Huber PE. Effects of CTGF Blockade on Attenuation and Reversal of Radiation-Induced Pulmonary Fibrosis. *J Natl Cancer Inst*. 2017; 109
56. Cho HY, Reddy SP, Yamamoto M, Kleeberger SR. The transcription factor NRF2 protects against pulmonary fibrosis. *FASEB J*. 2004; 18:1258–1260. [PubMed: 15208274]

Highlights

- Loss of Nrf2 inhibits the alveolar type 2 cell reparative process in irradiated lung
- Radiation-induced Np63 stem cell mobilization is inhibited in the Nrf2 null mouse
- Loss of Nrf2 promotes alveolar type 2 cell EMT.

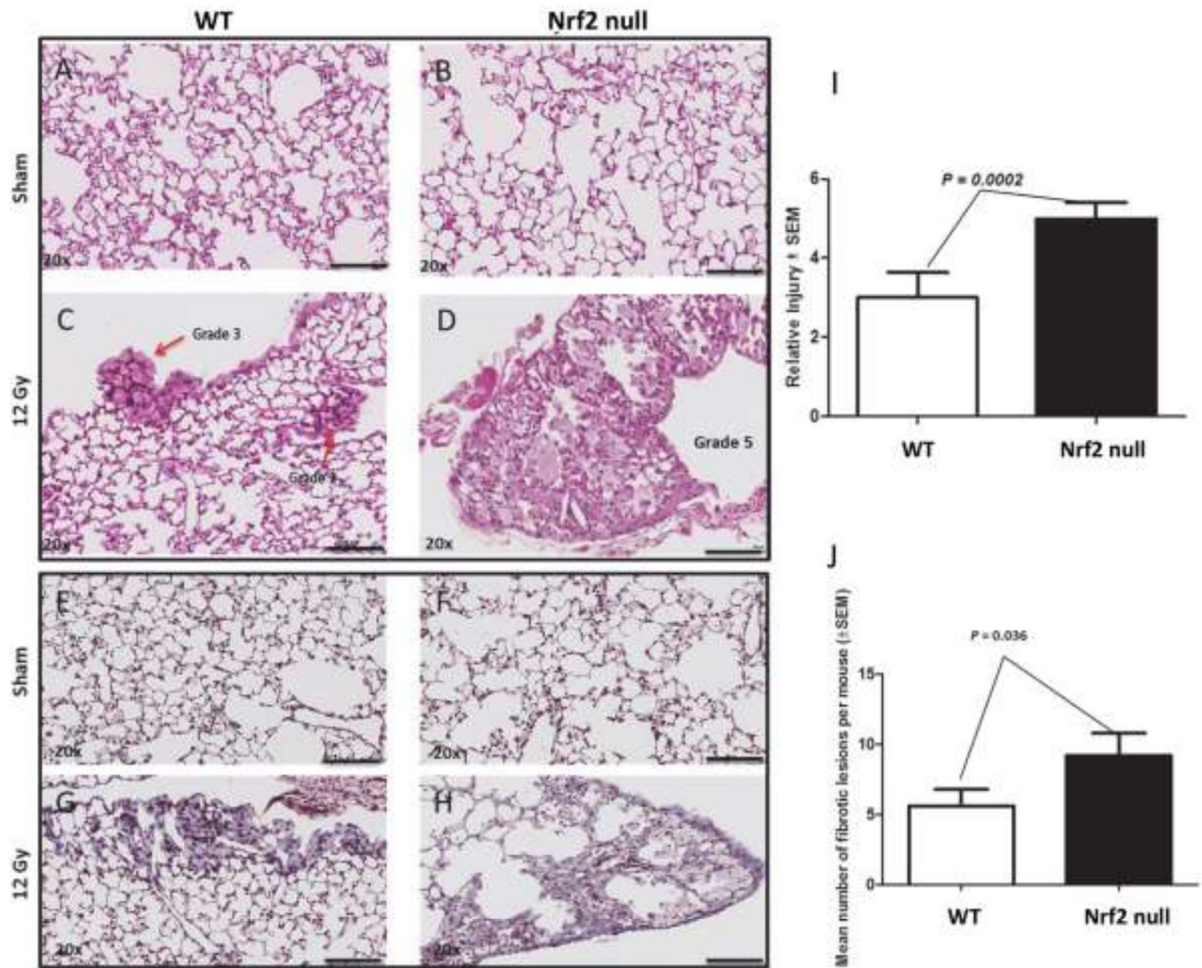


Figure 1.

Loss of Nrf2 potentiates radiation-induced tissue remodeling and collagen deposition. Male wild type (A, C, E, G) and Nrf2 null (B, D, F, H) mice were administered 0 (A, B, E, F) or 12 Gy (C, D, G, H) to the thorax and allowed to recover for 250 days. The degree of tissue remodeling was quantified from H&E sections (I, N = 112 fields, 10 mice) while collagen deposition was quantified from Masson's trichrome staining (J, N = 71 fields, 10 mice). Black bar = 100 μ m. Red arrow in panel C identifies tissue remodeling.

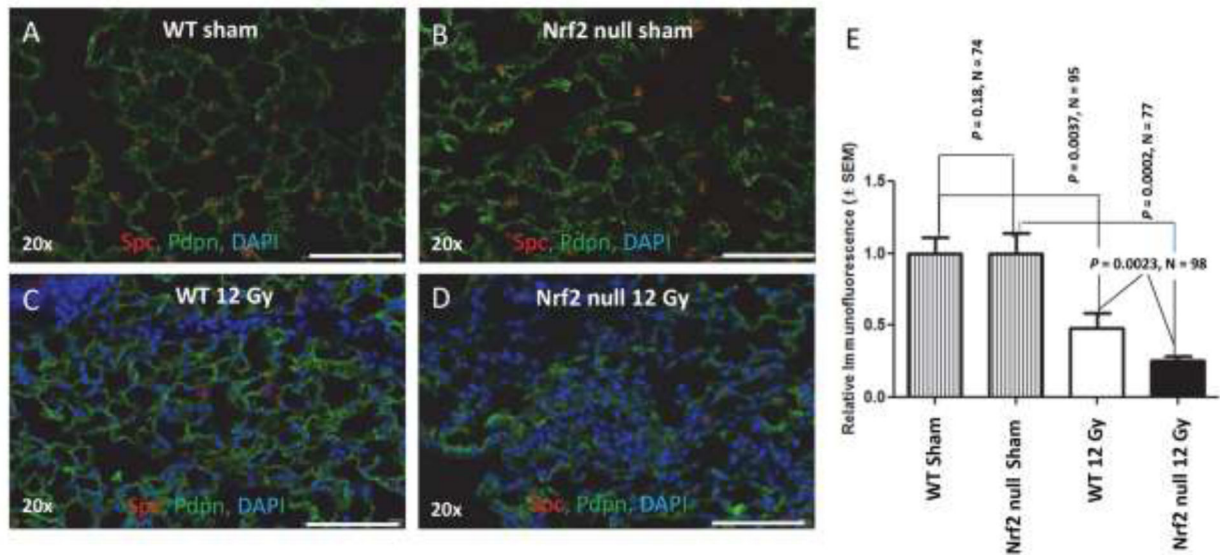


Figure 2.

Loss of Nrf2 potentiates radiation-induced injury to alveolar type 2 cells. The thorax of male wild type and Nrf2 null mice was administered 0 (A, B) or 12 Gy (C, D) and the mice allowed to recover for 250 days. Wide field whole slide scanning microscopy was used to image Pdpn immunofluorescence (green) in order to identify alveolar type 1 cells. Spc immunofluorescence (red) in alveoli was used to identify and quantify alveolar type 2 cells. DAPI staining identifies nuclei. E) Quantification of Spc immunofluorescent cells per field, corrected for DAPI staining. White bar 100 μ m.

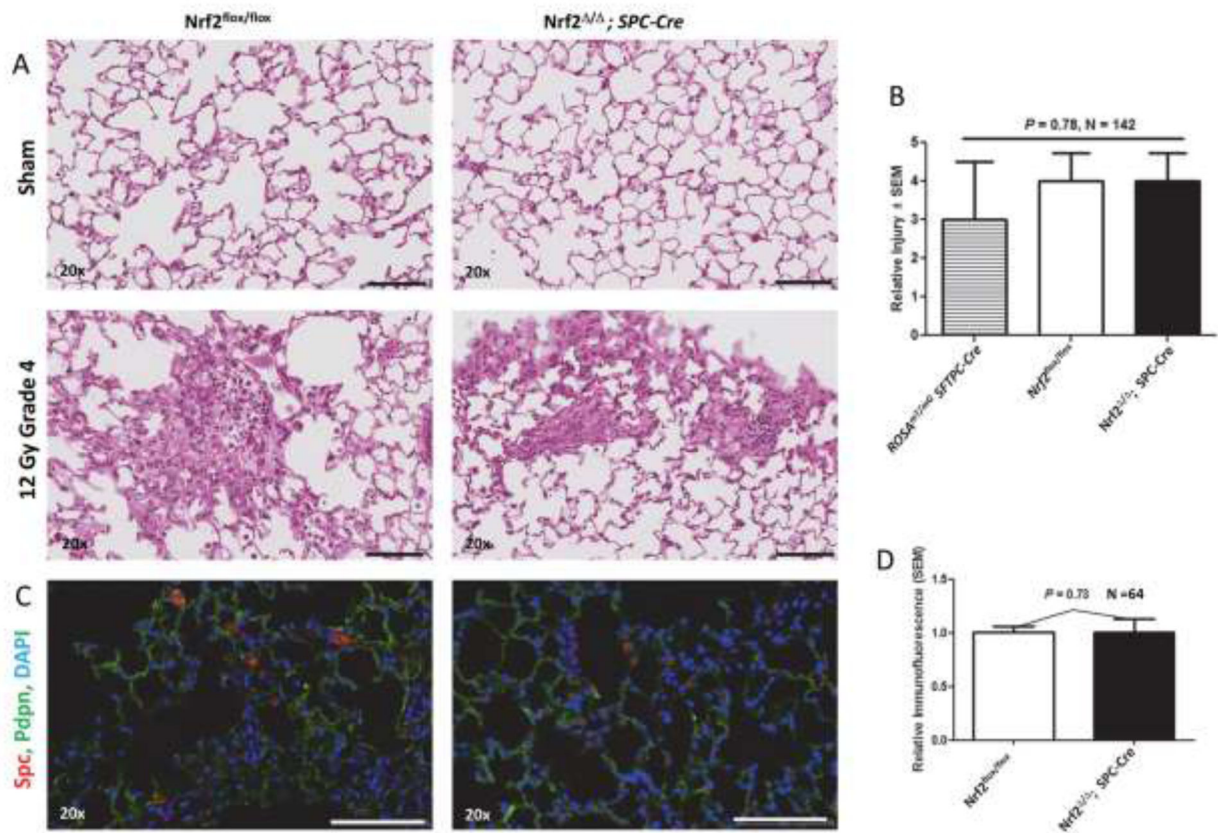


Figure 3.

Tissue remodeling and Spc immunofluorescence in sham (0 Gy) and irradiated (12 Gy) lung of Nrf2^{flox/flox} and Nrf2^{MA}; SPC-Cre mice 250 days after irradiation. A) Representative H&E stained sections. B) Quantification of tissue remodeling in irradiated ROSA^{mT/mG} SFTPC-Cre, Nrf2^{flox/flox} and Nrf2^{MA}; SPC-Cre mice. C) Representative sections immunostained for Spc (red) and Pdpn (green), and counter stained with DAPI, imaged using wide field whole slide scanner. microscopy. D) Quantification of relative Spc immunofluorescent cells per field corrected for DAPI staining. Black and white bars = 100 μ m.

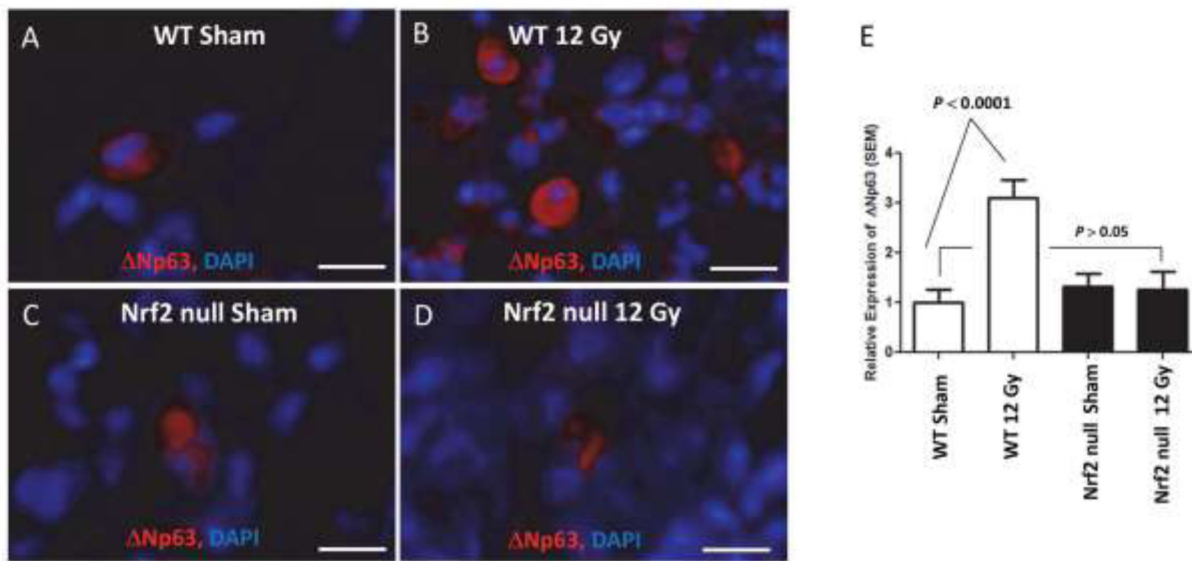


Figure 4. Loss of Nrf2 suppresses Δ Np63 progenitor cell mobilization in irradiated lung. The thorax of male wild type and Nrf2 null mice was administered 0 (A, B) or 12 Gy (C, D) and the mice allowed to recover for 250 days. Wide field whole slide scanning microscopy was used to image Δ Np63 immunofluorescence with DAPI counter staining. E) Quantification of Δ Np63 immunofluorescent cells per field corrected for DAPI staining. White bar = 10 μ M 40x.

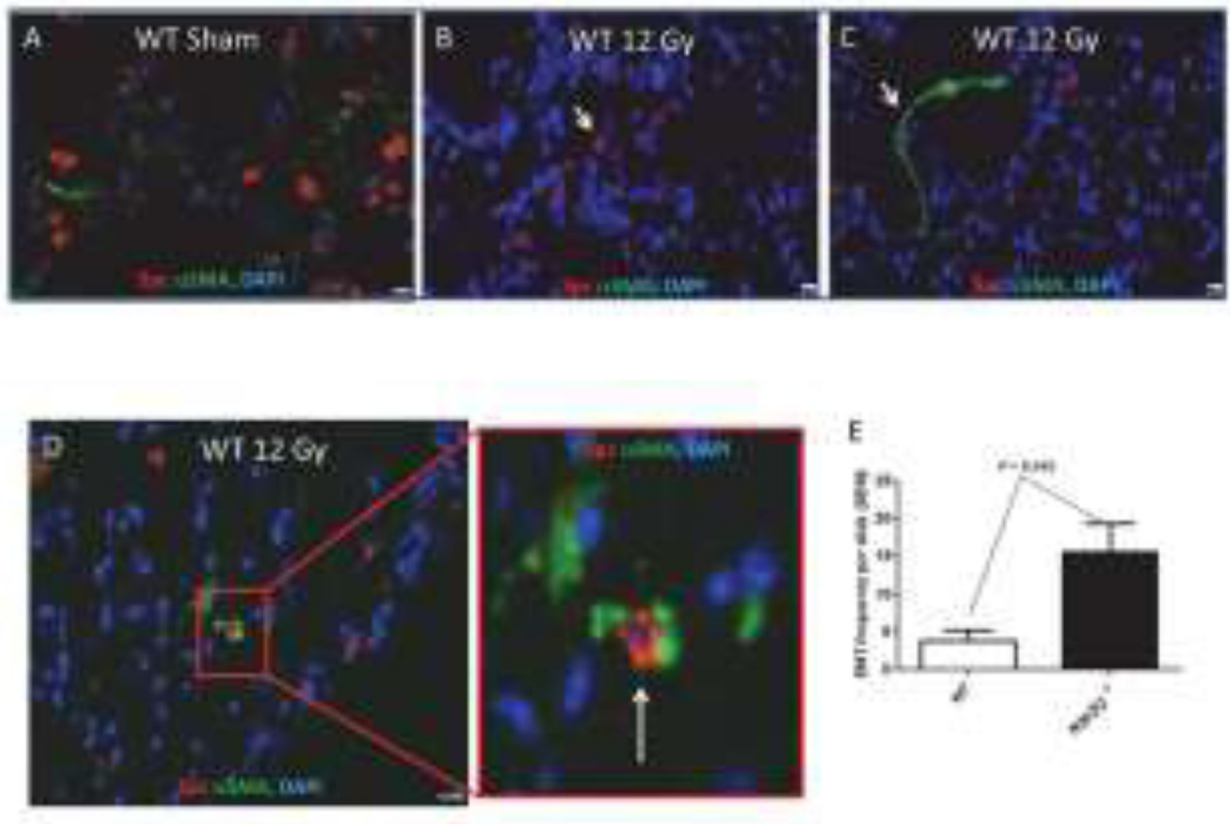


Figure 5.

Loss of Nrf2 increases EMT events in irradiated lung. The thorax of male wild type and Nrf2 null mice was administered 0 or 12 Gy and the mice were allowed to recover for 250 days. Wide field whole slide scanning microscopy was used to image Spc and αSMA immunofluorescence surrounding DAPI stained nuclei. A) A representative section from a sham treated wild type lung. B) A representative section from an irradiated wild type lung illustrating cells with only Spc immunofluorescence (white arrow). C) A representative section from an irradiated wild type lung illustrating cells with only αSMA immunofluorescence (white arrow). D) A representative section from an irradiated wild type lung illustrating a cell with both Spc and αSMA immunofluorescence (white arrow). E) The frequency of EMT events in wild type and Nrf2 null lung sections obtained from 8 mice. EMT events are defined as DAPI stained nuclei surround by both Spc and αSMA immunofluorescence. 40x, White bar = 10 μm.

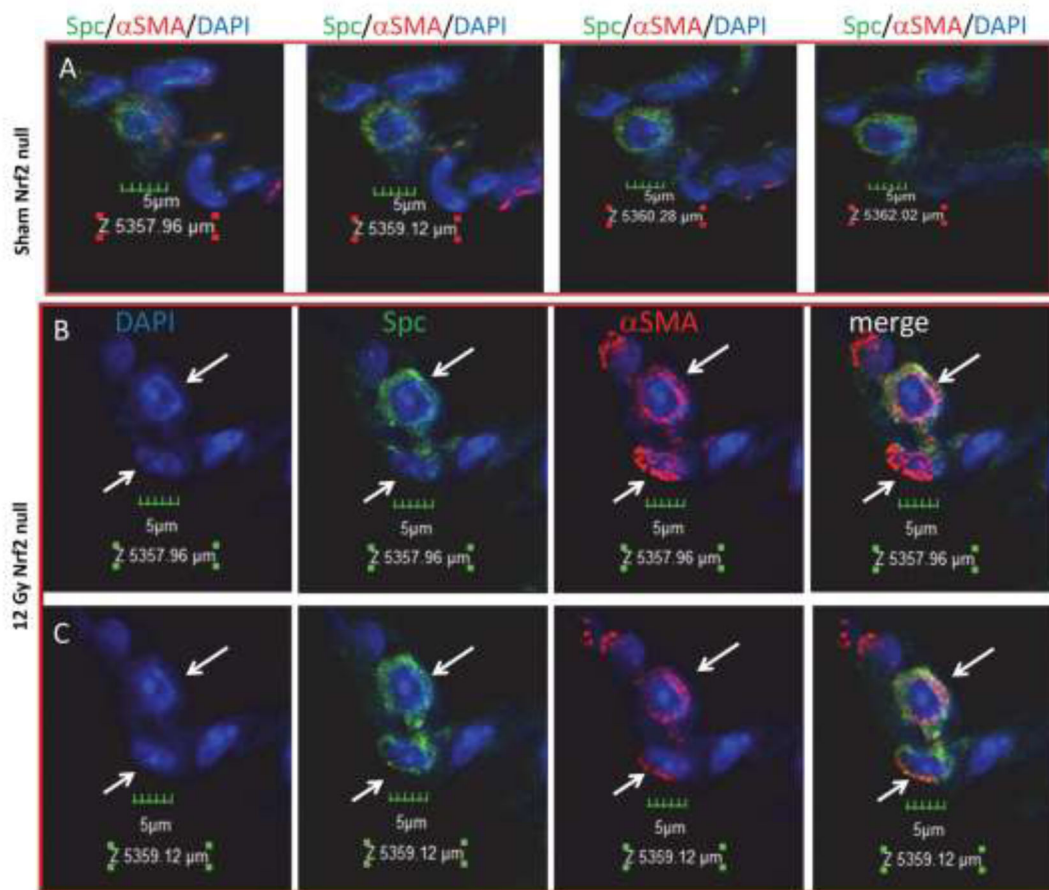


Figure 6.

Alveolar type 2 cell EMT. Thoraxes of Nrf2 null mice were administered 12 Gy and the mice were allowed to recover for 250 days. Confocal microscopy with Z stack imaging was used to capture Spc immunofluorescent (green) and α SMA immunofluorescent (red) cells. 40x with an additional 3x optical zoom. Panel A illustrates 4 of 9 - Z stack slices (0.58 μ m each) covering a total of 4.06 μ m. Six nuclei (blue, DAPI) are shown. None of the nuclei in Panel A co-express Spc and α SMA. Panel B illustrates two nuclei (blue, DAPI, white arrows) surrounded by both Spc (green) and α SMA (red), optical section Z5357.96 μ m, 40x with an additional 3x optical zoom. Panel C illustrates the same two nuclei as Panel B but at optical section Z5359.12 μ m, 40x with an additional 3x optical zoom.